Enhancing the Thermoelectric Properties of Layered Transition-Metal Dichalcogenides 2H-MQ2 (M = Mo, W; Q = S, Se, Te) by Layer Mixing: Density Functional Investigation

ARTICLE *in* CHEMISTRY OF MATERIALS · SEPTEMBER 2013

Impact Factor: 8.35 · DOI: 10.1021/cm402281n

4 AUTHORS, INCLUDING:

Changhoon Lee
North Carolina State University
181 PUBLICATIONS **1,671** CITATIONS

SEE PROFILE

Myung-Hwan Whangbo
North Carolina State University
704 PUBLICATIONS **14,990** CITATIONS

SEE PROFILE

Ji Hoon Shim
Pohang University of Science and Technology
68 PUBLICATIONS **1,525** CITATIONS

SEE PROFILE

CHEMISTRY OF MATERIALS

Article

pubs.acs.org/cm

Enhancing the Thermoelectric Properties of Layered Transition-Metal Dichalcogenides 2H-MQ_2 (M = Mo, W; Q = S, Se, Te) by Layer Mixing: Density Functional Investigation

Changhoon Lee,[†,‡] Jisook Hong,[†] Myung-Hwan Whangbo,*[,‡] and Ji Hoon Shim*[,†]

[†]Department of Chemistry, Pohang University of Science and Technology, Pohang 790-784, Korea

[‡]Department of Chemistry, North Carolina State University, Raleigh, North Carolina 27695-8204, United States

Supporting Information

ABSTRACT: We explored how to improve the thermoelectric properties of the layered transition-metal dichalcogenides 2H-MQ_2 (M = Mo, W; Q = S, Se, Te) by comparing the thermoelectric properties of hypothetical mixed-layer systems 2H-MQ_2/2H-MQ'_2, in which two different layers 2H-MQ_2 and 2H-MQ'_2 (Q, Q′ = S, Se, Te) alternate, with those of their pure components on the basis of density functional calculations. Our study predicts that the mixed-layer compounds MS_2/MTe_2 (M = Mo, W) strongly enhance the thermoelectric properties as a consequence of reducing the band gap and the interlayer van der Waals interactions. The layer-mixing is predicted to be a promising way of improving the thermoelectric properties of 2H-MQ_2.

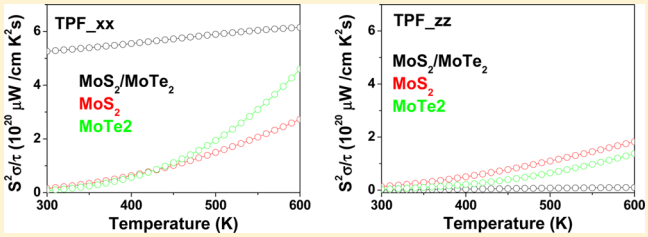

KEYWORDS: *thermoelectric property, layered transition-metal dichalcogenide, layer mixing, density functional calculation*

1. INTRODUCTION

The layered dichalcogenides of Group 6 elements, 2H-MQ_2 (M = Mo, W; Q = S, Se, Te), mostly crystallize in a space group $P6_3/mmc$,[1] in which the MQ_2 layers made up of edge-sharing MQ_6 trigonal prisms (Figure 1a,b) are stacked along the *c*-direction. (Hereafter the "2H" notation will be suppressed for simplicity.) These dichalcogenides have attracted much attention because of their anisotropic thermoelectric property,[2] charge density wave,[3] and superconductivity.[4−8] These dichalcogenides can be intercalated with various metal ions, which greatly affects their optical[9] and electrical[10−15] properties (e.g., n-type or p-type). The dichalcogenides MQ_2 (M = Mo,W; Q = S, Se, Te) are good candidates for thermoelectric applications because of their high Seebeck coefficients (S) and low thermal conductivities (κ).[10,16] The goodness of a thermoelectric material is judged by the figure of merit, $ZT = S^2\sigma T/\kappa$, where σ is the conductivity at a given temperature *T*. It is challenging to find a material with large ZT since the factors affecting it (i.e., S, σ, and κ) have conflicting properties.[17] The aim of the present work is to search for a way of improving the thermoelectric properties of layered MQ_2 compounds on the basis of the density functional theory (DFT) calculations. The electronic structures of layered MQ_2 systems around their band gaps are sensitively affected by the interlayer Q···Q van der Waals (vdW) interactions, and this effect becomes stronger as Q changes from S to Se to Te.[18] In a hypothetical mixed-layer system MQ_2/MQ'_2 (Q = S, Q′ = Se; Q = S, Q′ = Te; Q = Se, Q′ = Te) in which the MQ_2 and MQ'_2 layers alternate along the stacking direction (Figure 1c), the Q···Q′ vdW interactions could be weaker than the Q′···Q′ vdW interactions of pure MQ'_2. The thermoelectric properties of a semiconductor MQ_2 are strongly influenced in its electronic structure around the band gap and hence on the interlayer vdW interactions. Thus, one might speculate that the thermoelectric properties of MQ_2/MQ'_2 can differ considerably from those of pure MQ_2 or pure MQ'_2. Therefore, it is of interest and importance to examine if the construction of a mixed-layer system MQ_2/MQ'_2 is a way of improving the thermoelectric property of a layered MQ_2. In the present work, we show that this is indeed the case by comparing the thermoelectric properties of pure MQ_2 (M = Mo, W; Q = S, Se, Te) with those of hypothetical mixed-layer MS_2/MSe_2, MS_2/MTe_2, and MSe_2/MTe_2 (M = Mo, W) on the basis of first-principles DFT calculations.

2. COMPUTATIONAL DETAILS

WTe_2 crystallizes in a space group $Pnm2_1$,[1f] although its local structure is very similar to those of WQ_2 (Q = S, Se) and MoQ_2 (Q = S, Se, Te) that crystallize in a space group $P6_3/mmc$. In our study of pure WTe_2 phase, its structure will be assumed to crystallize in $P6_3/mmc$ for the purpose of comparison with WS_2 and WSe_2. Table 1 summarizes the structural parameters of MQ_2 we examined. Our DFT calculations employed the frozen-core projector augmented wave (PAW) method[19,20] encoded in the Vienna ab initio simulation package (VASP).[21] Unless specified otherwise, the generalized-gradient approximation (GGA)[22] of Perdew, Burke, and Ernzerhof (PBE) is used for the exchange-correlation functional with the plane-wave-cutoff energy of 450 eV. The interlayer Q···Q′ or Q···Q interactions in MQ_2 and mixed layer MQ_2/MQ'_2 are vdW interactions in nature, which are overestimated in the simple GGA

Received: July 10, 2013
Revised: August 19, 2013
Published: August 22, 2013

   dx.doi.org/10.1021/cm402281n | *Chem. Mater.* 2013, 25, 3745−3752

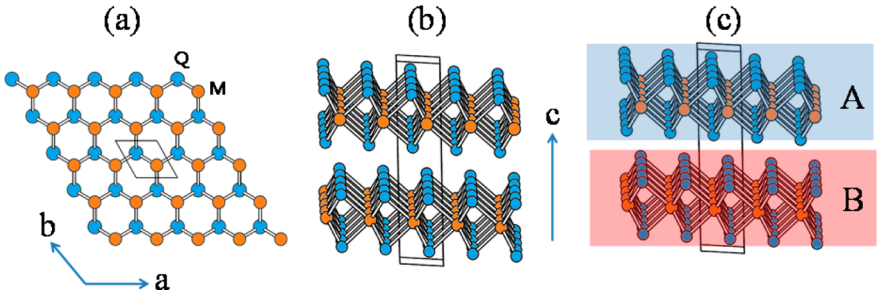

Figure 1. (a, b) Top and side views of the crystal structure of 2H-MQ_2, where M = Mo, W, and Q = S, Se, Te. The scarlet and blue circles represent metal and chalcogen atoms, respectively. (c) The side view of the mixed-layer MQ_2/MQ'_2 in which two different layers MQ_2 (A) and MQ'_2 (B) alternate along the stacking direction.

Table 1. Structural Parameters *a*, *c*, and z_Q of MQ_2[a] and Their Calculated Electronic Band Gaps E_g (eV) Obtained by the GGA Calculations[b]

	a (Å)	*c* (Å)	z_Q	M-Q (Å)	E_g
WS_2	3.1532	12.323	0.6225	2.405	0.97
WSe_2	3.282	12.960	0.6211	2.526	0.99
WTe_2	3.600	13.970	0.6211	2.751	0.82
MoS_2	3.169	12.324	0.6230	2.408	0.89
$MoSe_2$	3.289	12.927	0.6210	2.527	0.83
$MoTe_2$	3.519	13.964	0.6250	2.678	0.74

[a]Space group $P6_3/mmc$. [b]Here z_Q refers to the *z*-coordinate of the chalcogen Q (4h site).

method. Thus, in our study of MQ_2 and mixed layer MQ_2/MQ'_2 systems, we employed the vdW-DF scheme[23] so as to better describe their interlayer interactions. The structures of the pure MQ_2 (M = Mo, W, and Q = S, Se, Te) as well as mixed-layer MS_2/MSe_2, MS_2/MTe_2, and MSe_2/MTe_2 (M = Mo, W) compounds were optimized using a set of 200 k-points for the irreducible Brillouin zone, and the self-consistent-field convergence thresholds of 10^{-5} eV and 0.001 eV/Å for the total electronic energy and force, respectively. The optimized structural parameters of the MQ_2 compounds are listed in Supporting Information, Table S1, and those of the mixed-layer compounds MQ_2/MQ'_2 in Table 2, which have a lower-symmetry hexagonal structure (space group $P\bar{6}m2$).

The BoltzTrap code[24] was employed to calculate the thermoelectric properties of all pure and mixed-layer MQ_2 systems; it solves the semiclassical Boltzmann equation using the rigid band approach.[25] This method has been successful in calculating transport properties and predicting the optimal doping levels for thermoelectric materials.[26−29] To ensure the convergence of the calculated thermoelectric properties, the irreducible Brillouin zone was sampled by a set of 4,000 k-points. The BoltzTrap code allows one to calculate the electrical conductivity σ, the Seebeck coefficient *S*, and the thermoelectric power factors (TPFs) $S^2\sigma/\tau$ under the assumption that the relaxation times τ is energy-independent. We employ the latter assumption because there is currently no detailed theory of τ for MQ_2, MS_2/MSe_2, MS_2/MTe_2, and MSe_2/MTe_2 (M = Mo, W). Nevertheless, we note that the thermoelectric properties of numerous systems have been explained by using this assumption.[30] All thermoelectric property calculations for the pure MQ_2 and mixed-layer MQ_2/MQ'_2 compounds were based on the DFT electronic structures of their optimized crystal structures.

3. ELECTRONIC STRUCTURE OF PURE AND MIXED-LAYERED MQ_2

The electronic band structures of pure MQ_2 with the experimental crystal structures were calculated along the symmetry points Γ-M-K-Γ-Z in the Brillouin zone, where Γ, M, K, and Z represent the wave vector points (0, 0, 0), (1/2, 0, 0), (1/3, 1/3, 0), and (0, 0, 1/2) in the first Brillouin zone of the reciprocal lattice, respectively. The density of states (DOS) and band dispersion plots calculated for MoQ_2 (Q = S, Se, Te) are summarized in Figure 2, and those for WQ_2 (Q = S, Se, Te) in Figure 3. We also calculated the electronic structures of the optimized crystal structures by using the vdW-DF scheme to find that they are very similar to those of the experimental structures. The DOS and band dispersion plots calculated for the optimized MQ_2 (M = Mo, W, and Q = S, Se, Te) are summarized in Supporting Information, Figures S1 and S2. Each MQ_2 has an indirect band gap with the conduction band minimum (CBM) around the midpoint along the Γ−K line and the valence band maximum (VBM) at the Γ point. The calculated indirect band gaps of MoQ_2 and WQ_2, listed in Table 1, are in agreement with those reported in the previous theoretical studies.[31] The band dispersion relations of Figure 2 and 3 show that the width of the valence bands decreases slightly on going from S to Se to Te.

The electronic structures calculated for the mixed-layer MS_2/MSe_2, MS_2/MTe_2, and MSe_2/MTe_2 are summarized in Figure 4 for M = Mo, and in Figure 5 for M = W. The general features of the electronic structures of each layer (MQ_2 or MQ'_2) remain unchanged by the layer mixing, but those around the VBM and CBM do not. Analysis of these DOS and band dispersion plots leads to the following observations:

Table 2. Structural Parameters *a*, *c*, z_Q, $z_{Q'}$, M-Q and M-Q′ as well as the Band Gaps E_g (eV) of the Mixed-Layer Compounds MS_2/MSe_2, MS_2/MTe_2, and MSe_2/MTe_2 (M = Mo, W) with Space Group $P\bar{6}m2$ Obtained from the J. Klimes's vdW-DFT Calculations[a]

	a (Å)	*c* (Å)	z_Q (2h)	$z_{Q'}$ (2i)	M-Q (Å)	M-Q′ (Å)	E_g
$MoS_2/MoSe_2$	3.2575	12.8090	0.8789	0.3673	2.438	2.535	0.63
$MoS_2/MoTe_2$	3.3696	13.3565	0.8864	0.3588	2.467	2.712	
$MoSe_2/MoTe_2$	3.4448	13.7123	0.8806	0.3645	2.576	2.722	0.52
WS_2/WSe_2	3.2571	12.8926	0.8795	0.3676	2.439	2.540	0.79
WS_2/WTe_2	3.3665	13.4108	0.8867	0.3583	2.467	2.718	
WSe_2/WTe_2	3.4433	13.7683	0.8808	0.3644	2.577	2.727	0.58

[a]Here z_Q and $z_{Q'}$ refer to the *z*-coordinates of the lighter and heavier chalcogen atoms Q and Q′, respectively.

dx.doi.org/10.1021/cm402281n | Chem. Mater. 2013, 25, 3745−3752

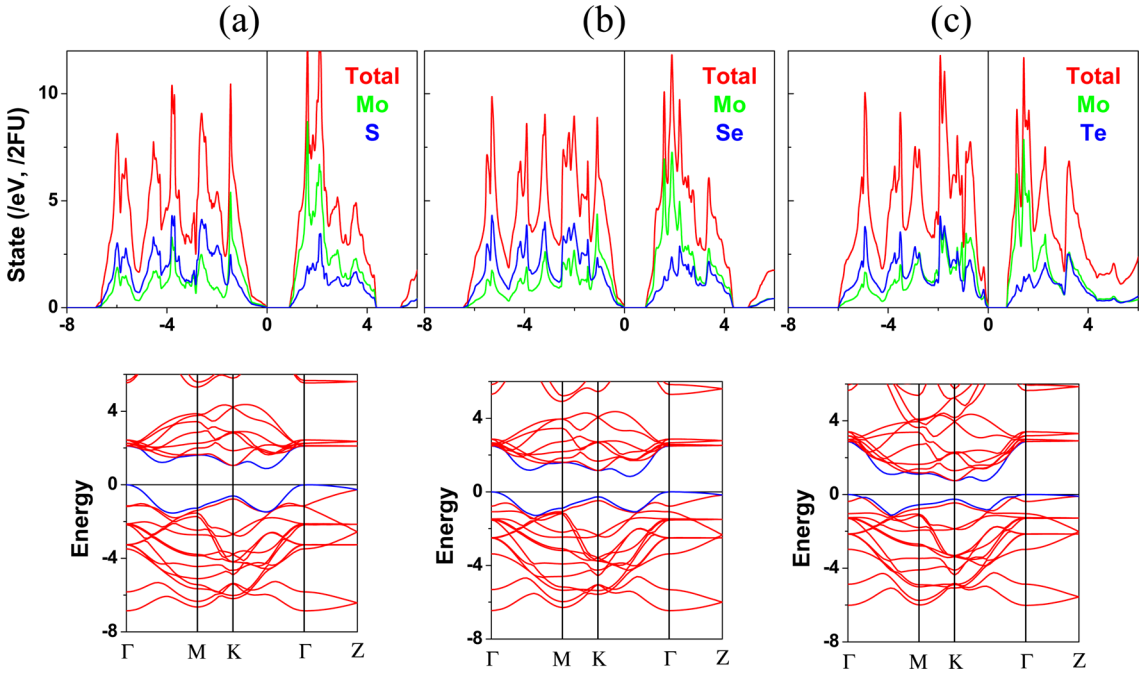

Figure 2. DOS (upper panel) and band dispersion (lower panel) plots calculated for MoQ_2: (a) MoS_2, (b) $MoSe_2$, and (c) $MoTe_2$.

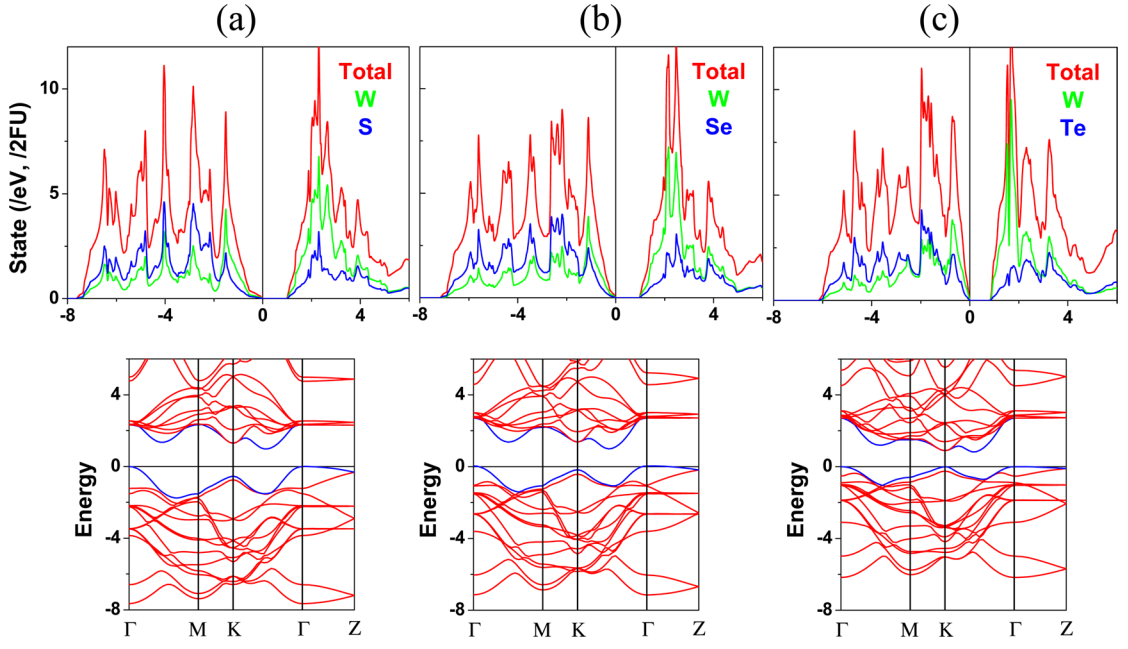

Figure 3. DOS (upper panel) and band dispersion (lower panel) plots calculated for WQ_2: (a) WS_2, (b) WSe_2, and (c) WTe_2.

(a) The existence of a band gap is clear for MS_2/MSe_2 and MSe_2/MTe_2 (M = Mo, W), but is unclear for MS_2/MTe_2 (M = Mo, W). Since the DFT calculation with the PBE functional usually underestimates a band gap, we carried out the calculations with the hybrid functional HSE06[32−34] resulting in the band gaps of 0.32 eV for WS_2/WTe_2 and 0.03 eV for $MoS_2/MoTe_2$ (see Supporting Information, Figure S3).

(b) All the mixed-layer systems MS_2/MSe_2, MS_2/MTe_2, and MSe_2/MTe_2 (M = Mo, W) have their CBM at K points and the almost degenerate VBM at the K and M points (K and Γ points for MS_2/MSe_2) and hence have a pseudodirect band gap. These band gaps are smaller than those of their pure components (Table 1 and 2). In particular, the MS_2/MTe_2 (M = Mo, W) system has a very small band gap. This finding is explained in terms of the schematic DOS diagram depicted for the valence and conduction bands in Figure 6 for a mixed-layer structure in which two different layers A and B alternate. When the layer A has a more electronegative chalcogen atom than does the layer B, the VBM and CBM of the layer A are lowered in energy with respect to those of the layer B. Thus, the band gap E_g of a mixed-layer structure is smaller than those of its pure components, and the smallest band gap is expected when the two different chalcogen atoms have the largest difference in the electronegativity. This is indeed the case, as found for MS_2/MTe_2 (M = Mo, W).

dx.doi.org/10.1021/cm402281n | *Chem. Mater.* 2013, 25, 3745−3752

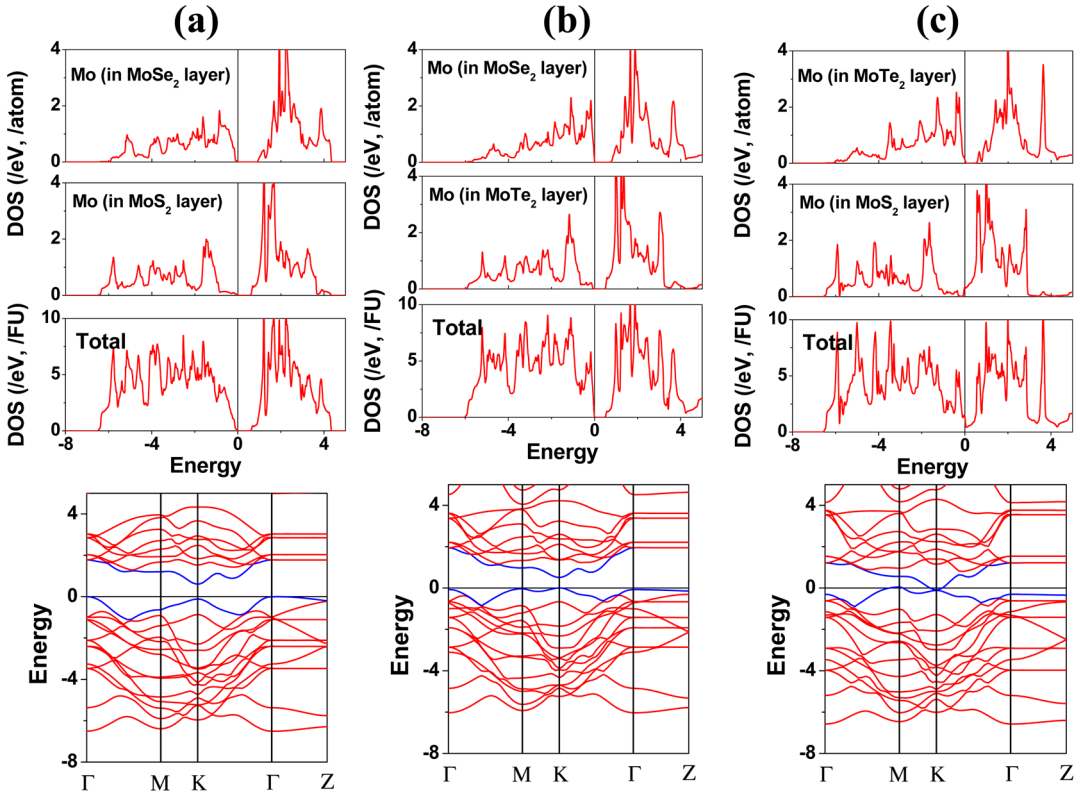

Figure 4. DOS (upper panel) and band dispersion (lower panel) plots calculated for the mixed-layer compounds: (a) $MoS_2/MoSe_2$, (b) $MoS_2/MoTe_2$, and (c) $MoSe_2/MoTe_2$.

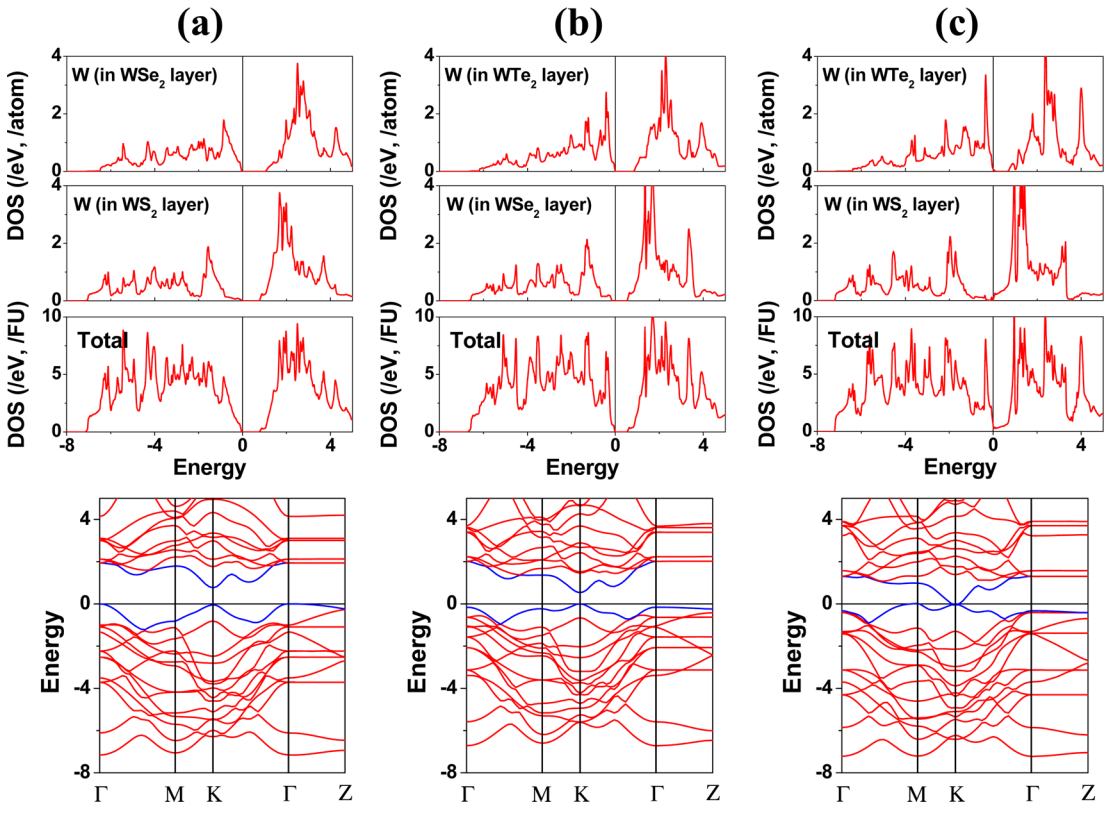

Figure 5. DOS (upper panel) and band dispersion (lower panel) plots calculated for the mixed-layer compounds: (a) WS_2/WSe_2, (b) WS_2/WTe_2, and (c) WSe_2/WTe_2.

(c) The MoS_2 monolayer is regarded as a candidate for optical device applications because of its direct and controllable band gap.[33−38] For similar reasons, the mixed-layer systems would be promising for optical device applications.

dx.doi.org/10.1021/cm402281n | *Chem. Mater.* 2013, 25, 3745−3752

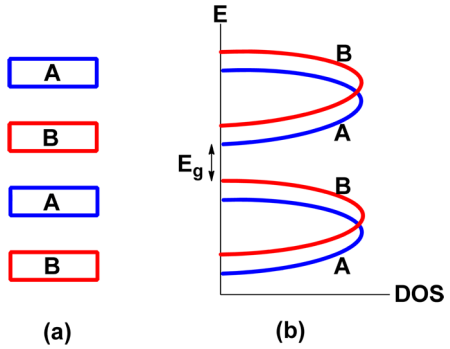

Figure 6. Schematic diagram illustrating why the band gap of a mixed-layer system MQ_2/MQ'_2 is smaller than those of its pure components. In the mixed-layer structure shown in (a), the layer A is assumed to have a more electronegative chalcogen atom than does the layer B. Thus, the VBM and CBM of the layer A are lowered in energy with respect to those of the layer B as depicted in (b), leading to a small band gap E_g.

(d) The *c*-axis length of each optimized mixed-layer MQ_2/MQ'_2 is almost the same as the average of the optimized *c*-axis lengths of its pure components. Unlike the case of its pure components, each mixed-layer MQ_2/MQ'_2 has a pseudodirect band gap, namely, the CBM at the K point and the degenerate VBM at the K as well as M (or Γ) points. The Q np and Q′ n′p orbitals differ in energy. In general, the orbital interaction between different levels is weaker than that between identical levels. Thus, the interlayer vdW interaction would be slightly weakened in mixed-layer MQ_2/MQ'_2 compounds. As a consequence, the electronic structure of a mixed-layer MQ_2/MQ'_2 becomes more two-dimensional in character than that of its pure component MQ_2 or MQ'_2.

4. THERMOELECTRIC PROPERTIES

Our analysis shows that the electronic structures around the band gaps of the mixed-layer compounds of MS_2/MTe_2 (M = Mo, W) exhibit drastic changes from those of their pure components MS_2 and MTe_2; MS_2/MTe_2 has a strongly reduced band gap and an enhanced density of states around the Fermi level. Let us now examine how the thermoelectric properties of MS_2/MTe_2 differ from those of its components MS_2 and MTe_2. Since the MQ_2, MQ'_2, and MQ_2/MQ'_2 systems have a layered structure and hence possess anisotropic electronic structures, one needs to evaluate the in-plane and out-of-plane thermoelectric properties. Figure 7a and Figure 8a summarize the dependence of the in-plane Seebeck coefficients S_{xx} on chemical potential μ calculated for MS_2, MTe_2, and MS_2/MTe_2 at 300 K, and that of the corresponding out-of-plane Seebeck coefficients S_{zz} is shown in Figure 7b and Figure 8b. The μ-dependence of the Seebeck coefficients *S* for WS_2, WTe_2, MoS_2, and $MoTe_2$ (Figure 7a,b, and Figure 8a,b) present two peaks at $\mu \approx \pm 0.1$ eV. The maximum Seebeck coefficients are 1500 and 1600 μV/K for WS_2 and MoS_2, respectively, and 1300 and 1400 μV/K for WTe_2 and $MoTe_2$, respectively. Thus the Seebeck coefficients are slightly larger for the sulfides than the tellurides, which is related to the fact that the tellurides have higher electron densities around the Fermi level and a smaller band gap than do the sulfides. In contrast, the μ-dependence of the Seebeck coefficients calculated for WS_2/WTe_2 and $MoS_2/MoTe_2$ presents many peaks and is quite small compared with those of its pure components. The S 3p and Te 5p orbitals have a large difference in energy and orbital diffuseness, so that the interlayer S···Te vdW interactions become weak. This increases the DOS for the electronic states of the MTe_2 layer around the Fermi level hence leading to small Seebeck coefficients for WS_2/WTe_2 and $MoS_2/MoTe_2$.

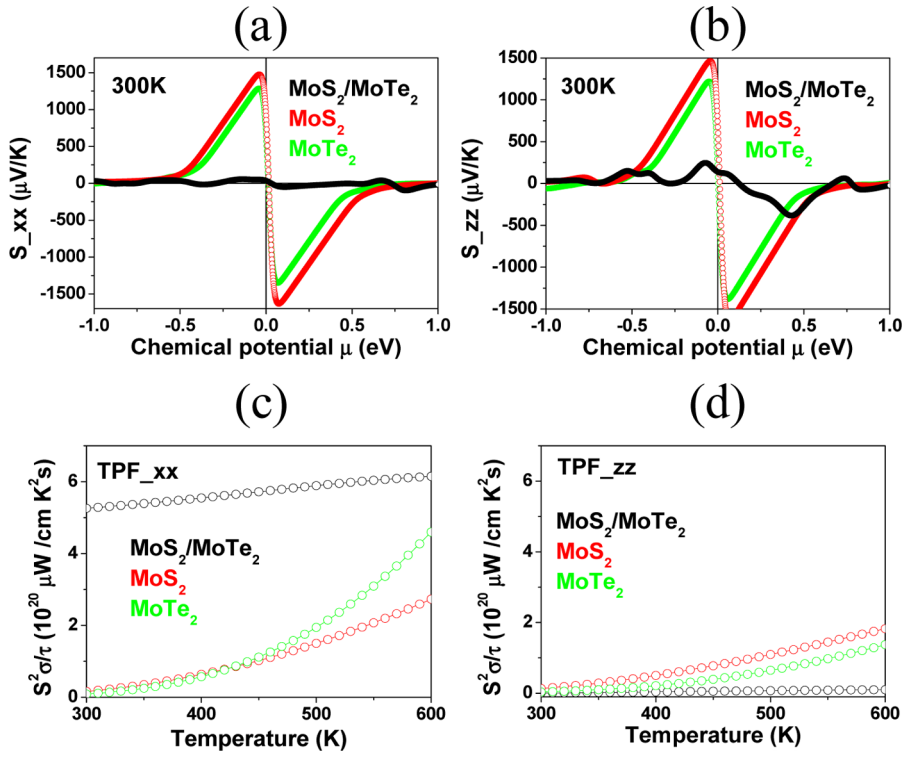

Figure 7. (a) In-plane and (b) out-of-plane Seebeck coefficients calculated for MoS_2, $MoTe_2$, and $MoS_2/MoTe_2$ as a function of the chemical potential μ. (c) The in-plane and (d) out-of-plane TPFs calculated for MoS_2, $MoTe_2$, and $MoS_2/MoTe_2$ as a function of temperature.

dx.doi.org/10.1021/cm402281n | *Chem. Mater.* 2013, 25, 3745−3752

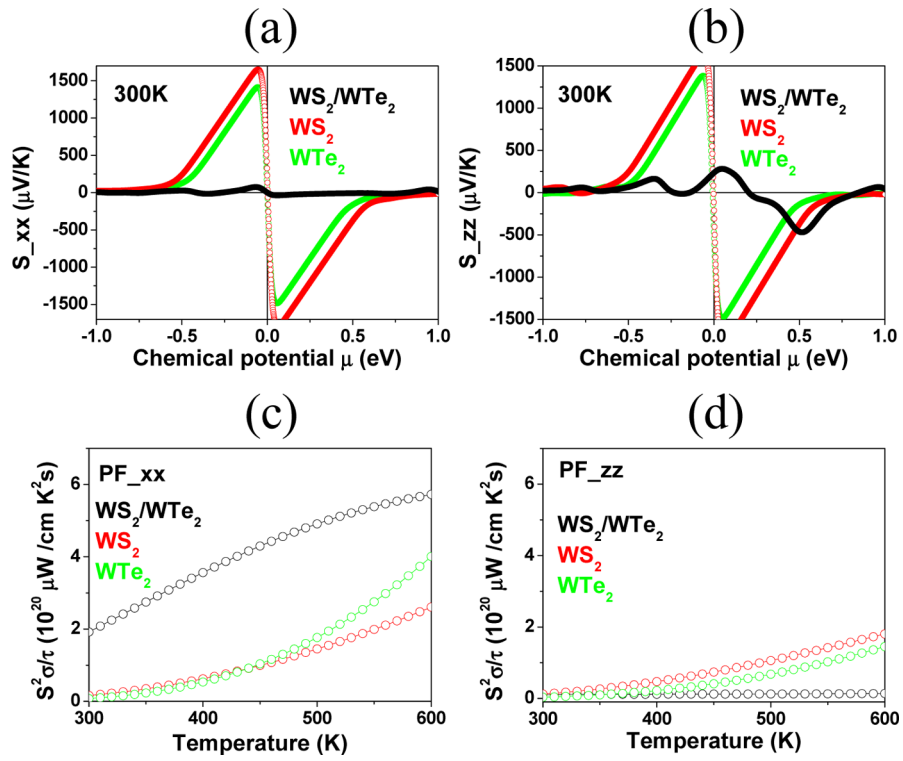

Figure 8. (a) In-plane and (b) out-of-plane Seebeck coefficients calculated for WS_2, WTe_2, and WS_2/WTe_2 as a function of the chemical potential μ. (c) The in-plane and (d) out-of-plane TPFs calculated for WS_2, WTe_2, and WS_2/WTe_2 as a function of temperature.

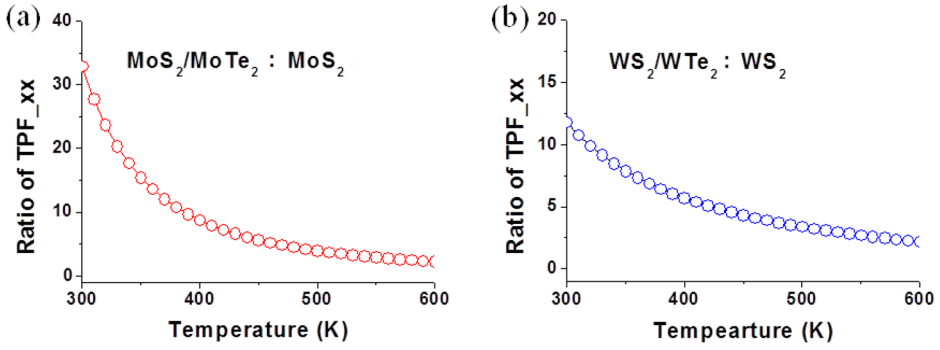

Figure 9. Ratio of the in-plane TPF of MS_2/MTe_2 to that of MS_2 as a function of temperature: (a) M = Mo and (b) M = W.

We note that the optimum power factor is generally found for the carrier concentration around $n_{eff} \approx 10^{19}-10^{20}$ cm^{-3} in the conventional semiconducting materials.[39] However, the carrier concentrations of bulk MQ_2 (M = Mo, W; Q = S, Te) compounds are usually in the range of $10^{15}\sim10^{18}$ cm^{-3} at the room temperature. Thus, in calculating the TPFs of Figure 7 and 8, we chose the carrier concentration in the range of $n_{eff} \approx 5 \times 10^{17}$ cm^{-3} for p-type doping cases. In these calculations the number of carriers is changed by varying the chemical potential and temperature; in the case of n-type doping, the Fermi level is raised, which corresponds to a positive chemical potential μ. For the p-type doping, the Fermi level is lowered and the corresponding μ is negative. Figure 7c and 7d show the in-plane and out-of-plane TPFs, $(S^2\sigma/\tau)_{xx}$ and $(S^2\sigma/\tau)_{zz}$, respectively, calculated for MoS_2, $MoTe_2$ and $MoS_2/MoTe_2$ as a function of temperature. The corresponding results obtained for WS_2, WTe_2 and WS_2/WTe_2 are summarized in Figure 8c and 8d. These results show that the in-plane TPF is much greater than the out-of-plane TPF for both MQ_2/MQ'_2 as well as its pure components MQ_2 and MQ'_2. Also, the out-of-plane TPF of MQ_2/MQ'_2 is negligible compared with those of its pure components MQ_2 and MQ'_2, which indicates that the anisotropy of TPF is much enhanced by the layer mixing. Clearly, the thermoelectric properties of MQ_2/MQ'_2 are dominated by the in-plane TPF.

Note that the in-plane TPFs of $MoS_2/MoTe_2$ and WS_2/WTe_2 are considerably greater than those of their pure components (Figure 9), despite the fact that their Seebeck coefficients are much smaller than those of the pure components. However, TPF also depends on the conductivity, namely, TPF $\propto S^2\sigma$. MS_2/MTe_2 (M = Mo, W) has a very small band gap, which makes its conductivity much higher than those of its pure components MQ_2 and MQ'_2 (see Figure 10). The conductivity has a stronger effect than does the Seebeck coefficient in controlling the magnitude of the TPFs of $MoS_2/MoTe_2$ and WS_2/WTe_2. Our results suggest that the layer mixing is a promising way of enhancing the thermoelectric properties of layered dichalcogenides MQ_2.

dx.doi.org/10.1021/cm402281n | Chem. Mater. 2013, 25, 3745−3752

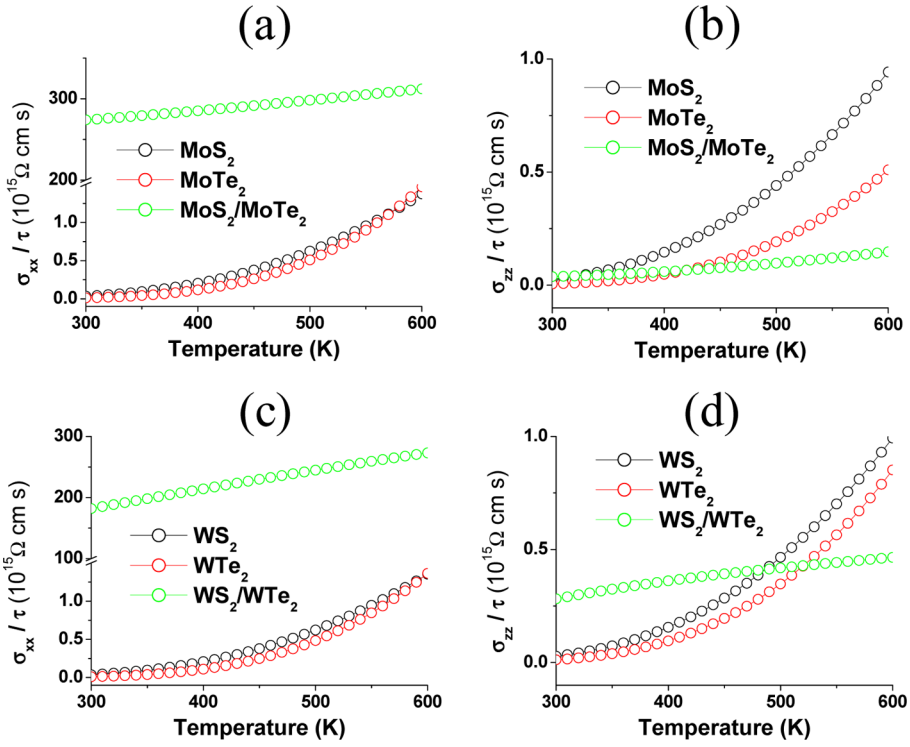

Figure 10. Conductivities calculated for the p-type doping cases of MS_2/MTe_2 (M = Mo, W), MS_2 and MTe_2 as a function of temperature. The in-plane and out-of-plane conductivities for M = Mo are presented in (a) and (b), respectively, and those for M = W in (c) and (d), respectively.

5. CONCLUSIONS

Pure dichalcogenides MQ_2 (M = Mo, W; Q = S, Se. Te) have an indirect band gap while the hypothetical mixed-layer compounds MS_2/MSe_2, MS_2/MTe_2, and MSe_2/MTe_2 (M = Mo, W) possess a pseudo-direct band gap. The TPFs of MS_2/MTe_2 (M = Mo, W) are strongly enhanced compared with those of their pure components, largely because their band gap is strongly reduced. Our study predicts that the thermoelectric properties of MQ_2 can be strongly improved by layer mixing. It would be of interest to test this prediction by fabricating the mixed-layer MS_2/MTe_2 (M = Mo, W) phases.

■ ASSOCIATED CONTENT

Supporting Information

Further details are given in Figures S1, S3, S4, and Table S2. This material is available free of charge via the Internet at http://pubs.acs.org.

■ AUTHOR INFORMATION

Corresponding Authors

*E-mail: mike_whangbo@ncsu.edu (M-H.W.).
*E-mail: jhshim@postech.ac.kr (J.H.S.).

Notes

The authors declare no competing financial interest.

■ ACKNOWLEDGMENTS

This research was supported by the computing resources of the NERSC center and the HPC center of NCSU. J.H.S. was supported by the National Research Foundation of Korea (NRF) funded by the Ministry of Education, Science and Technology (20110030147, 2013R1A1A2006416).

■ REFERENCES

(1) (a) Schutte, W. J.; de Boer, J. L.; Jellinek, F. *J. Solid State Chem.* **1987**, *70*, 207. (b) Whittingham, M. S.; Gamble, F. R. *Mater. Res. Bull.* **1975**, *10*, 363. (c) Petkov, V.; Billinge, S. J. L.; Larson, P.; Mahanti, S. D.; Vogt, T.; Rangan, K. K.; Kanatzidis, M. G. *Phys. Rev. B* **2002**, *65*, 092105. (d) Bronsema, K. D.; de Boer, J. L.; Jellinek, F. *Z. Anorg. Allg. Chem.* **1986**, *540*, 15. (e) Puotinen, D.; Newnham, R. E. *Acta Crystallogr.* **1961**, *14*, 691. (f) Brown, B. E. *Acta Crystallogr.* **1966**, *20*, 268.

(2) (a) Nevile, R. A.; Evans, B. L. *Phys. Status Solidi B* **1976**, *73*, 597. (b) Novoselov, K. S.; Jinag, D.; Schedin, F.; Booth, T. J.; Khotkevich, V. V.; Morozov, S. V.; Geim, A. K. *Proc. Natl. Acad. Sci. U.S.A.* **2005**, *102*, 10451. (c) Coleman, J. N.; et al. *Science* **2011**, *331*, 568. (d) Splendiani, A.; Sun, L.; Zhang, Y.; Li, T.; Kim, J.; Chim, C.; Galli, G.; Wang, F. *Nano Lett.* **2010**, *10*, 1271. (e) Böker, T.; Severin, R.; Müller, A.; Janowitz, C.; Manzke, R.; Voß, D.; Krüger, P.; Mazur, A.; Pollmann, J. *Phys. Rev. B* **2001**, *64*, 235305. (f) Remskar, M.; et al. *Science* **2001**, *292*, 479. (g) Mak, K. F.; Lee, C.; Hone, J.; Shan, J.; Heinz, T. F. *Phys. Rev. Lett.* **2010**, *105*, 136805. (h) Reshak, A. H.; Auluck, S. *Phys. Rev. B* **2005**, *71*, 155114. (i) He, J.; Wu, K.; Sa, R.; Li, Q.; Wei, Y. *App. Phys. let* **2010**, *96*, 082504.

(3) (a) Wilson, J. A. *Phys. Rev. B* **1979**, *19*, 6456. (b) Wilson, J. A.; DiSalvo, F. J.; Mahajan, S. *Adv. Phys.* **1975**, *24*, 117. (c) Ishihara, Y.; Nakada, I.; Suzuki, K.; Ichihara, M. *Solid State Commun.* **1984**, *50*, 657. (d) Suzuki, K.; Ichihara, M.; Nakada, I.; Ishihara, Y. *Solid State Commun.* **1984**, *52*, 743. (e) DiSalvo, F. J.; Rice, T. M. *Phys. Today* **1979**, *32*, 32. (f) Electronic Properties of Inorganic Quasi-one-dimensional Compounds. In *Physics and Chemistry of Materials with Low-dimensional Structures Series B*; Monceau, P., Ed.; D. Reidel: Dordrecht, The Netherlands, 1985; Parts 1 and 2.

(4) Amberger, E.; Polborn, K.; Grimm, P.; Dietrich, M.; Obst, B. *Solid State Commun.* **1978**, *26*, 943.

(5) Biberacher, W.; Schwenk, H. *Solid State Commun.* **1980**, *33*, 385.

(6) Ishihara, Y.; Nakada, I. *Solid State Commun.* **1982**, *42*, 579.

(7) Fuller, W. W.; Chaikin, P. M.; Ong, N. P. *Solid State Commun.* **1979**, *30*, 689.

(8) Gamble, F. R.; DiSalvo, F. J.; Klemm, R. A.; Geballe, T. H. *Science* **1970**, *168*, 568.

(9) Neville, R. A.; Evans, B. L. *Phys. Status Solidi B* **1976**, *73*, 597.
(10) Brixner, L. H. *J. Inorg, Nucl. Chem.* **1962**, *24*, 257.
(11) Brixner, L. H.; Teufer, G. *Inorg. Chem.* **1963**, *2*, 992.
(12) Bureau of Ships, Progress Report AD 1960, Vol. *265*, p 106 (unpublished).
(13) Conan, A.; Bonnet, A.; Amrouche, A.; Spiesser, M. *J. Phys. (Paris)* **1984**, *45*, 459.
(14) Troadec, J. P.; Bideau, D.; Guyon, E. *J. Phys. C: Solid State Phys.* **1981**, *14*, 4807.
(15) *Annual Review of Materials Science*; Vol. *3*, pp 147−170 (Volume publication date August 1973).
(16) (a) Guo, H.; Yang, T.; Wang, Y.; Zhang, Z. *arXiv*:1208.5941, **2012**. (b) Huang, X.; Zeng, Z.; Zhang, H. *Chem. Soc. Rev.* **2013**, *42*, 1934. (c) Hébert, S.; Kobayashi, W.; Muguerra, H.; Bréard, Y.; Raghavendra, N.; Gascoin, F.; Guilmeau, E.; Maignan, A. *Phys. Status Solidi A* **2013**, *210*, 69.
(17) Snyder, G. J.; Toberer, E. S. *Nat. Mater.* **2008**, *7*, 105.
(18) Canadel, E.; Jobic, S.; Brec, R.; Rouxel, J.; Whangbo, M.-H. *J. Solid State Chem.* **1992**, *99*, 189.
(19) Blöchl, P. E. *Phys. Rev. B* **1994**, *50*, 17953.
(20) Kresse, G.; Joubert, D. *Phys. Rev. B* **1999**, *59*, 1758.
(21) Kresse, G.; Furthmüller, J. *Phys. Rev. B* **1996**, *54*, 11169.
(22) Perdew, J. P.; Burke, K.; Ernzerhof, M. *Phys. Rev. Lett.* **1996**, *77*, 3865.
(23) (a) Klimes, J.; Bowler, D. R.; Michelides, A. *J. Phys.: Condens. Matter* **2010**, *22*, 022201. (b) Klimes, J.; Bowler, D. R.; Michelides, A. *Phys. Rev. B* **2011**, *83*, 195131.
(24) Madsen, G. K. H.; Singh, D. *J. Comput. Phys. Commun.* **2006**, *175*, 67.
(25) Boker, T.; Severin, R.; Muller, A.; Janowitz, C.; Manzke, R.; Vob, D.; Kruger, P.; Mazur, A.; Pollmann, J. *Phys. Rev. B* **2001**, *64*, 235305.
(26) Scheidemantel, T. J.; Ambrosch-Draxl, C.; Thonhauser, T.; Badding, J. V.; Sofo, J. O. *Phys. Rev. B* **2003**, *68*, 125210.
(27) Madsen, G. K. H. *J. Am. Chem. Soc.* **2006**, *128*, 12140.
(28) Chaput, L.; Pécheur, P.; Tobola, J.; Scherrer, H. *Phys. Rev. B* **2005**, *72*, 085126.
(29) Gao, X.; Uehara, K.; Klug, D. D.; Patchkovskii, S.; Tse, J. S.; Tritt, T. M. *Phys. Rev. B* **2005**, *72*, 125202.
(30) (a) Ong, K. P.; Singh, D. J.; Wu, P. *Phys. Rev. B* **2011**, *83*, 115110. (b) Parker, D.; Du, M. -H.; Singh, D. J. *Phys. Rev. B* **2011**, *83*, 245111. (c) Zhang, L.; Singh, D. J. *Phys. Rev. B* **1993**, *47*, 13164. (d) Singh, D. J. *Phys. Rev. B* **2010**, *81*, 195217. (e) Zhang, L.; Du, M.-H.; Singh, D. J. *Phys. Rev. B* **2010**, *81*, 075117. (f) Madsen, G. K. H.; Schwarz, K.; Blaha, P.; Singh, D. J. *Phys. Rev. B* **2003**, *68*, 125212. (g) Scheidemantel, T. J.; Ambrosch-Draxl, C.; Thonhauser, T.; Badding, J. V.; Sofo, J. O. *Phys. Rev. B* **2003**, *68*, 125210. (h) Bertini, L.; Gatti, C. *J. Chem. Phys.* **2004**, *121*, 8983. (i) Lykke, L.; Iversen, B. B.; Madsen, G. K. H. *Phys. Rev. B* **2006**, *73*, 195121. (j) Wang, Y.; Chen, X.; Cui, T.; Niu, Y.; Wang, Y.; Wang, M.; Ma, Y.; Zou, G. *Phys. Rev. B* **2007**, *76*, 155127. (k) Diakhate, M. S.; Hermann, R. P.; Möchel, A.; Sergueev, I.; Søndergaard, M.; Christense, M.; Verstraete, M. J. *Phys. Rev. B* **2011**, *84*, 125210. (l) Guo, H.; Yang, T.; Tao, P.; Wang, Y.; Zhang, Z. *J. Appl. Phys.* **2013**, *113*, 013709. (m) Pulikkotil, J. J.; Singh, D. J.; Auluck, S.; Saravanan, M.; Misra, D. K.; Dhar, A.; Budhani, R. C. *Phys. Rev. B* **2012**, *86*, 155204. (n) Si, H. G.; Wang, Y. X.; Yan, Y. L.; Zhang, G. B. *J. Phys. Chem.* **2012**, *116*, 3956. (o) Xu, B.; Long, C. G.; Wang, Y.; Yi, L. *Chem. Phys. Lett.* **2012**, *529*, 45. (p) Aliabad, H. A. R.; Ghazanfari, M.; Ahmad, I.; Saeed, M. A. *Comput. Mater. Sci.* **2012**, *65*, 509. (q) Yang, X. H. *J. Appl. Phys.* **2012**, *111*, 033701. (r) Pardo, V.; Botana, A.; Baldomir, D. *Phys. Rev. B* **2012**, *86*, 165114.
(31) (a) Kumar, A.; Ahluwalia, P. K. *Eur. Phys. J. B* **2012**, *85*, 186. (b) Dawson, W. G.; Bullett, D. W. *J. Phys. C: Solid State Phys.* **2000**, *20*, 6159.
(32) Becke, A. D. *J. Chem. Phys.* **1993**, *98*, 1372.
(33) Heyd, J.; Scuseria, G. E.; Ernzerhof, M. *J. Chem. Phys.* **2003**, *118*, 8207; *J. Chem. Phys.* **2006**, *124*, 219906.
(34) Marsman, M.; Paier, J.; Stroppa, A.; Kresse, G. *J. Phys.: Condens. Matter* **2009**, *20*, 201.
(35) Novoselov, K.; Jiang, D.; Schedin, F.; Booth, T.; Khotkevich, V.; Morozov, S.; Geim, A. *Proc. Natl. Acad. Sci.U.S.A.* **2005**, *102*, 10451.
(36) Coleman, J. N.; et al. *Science* **2011**, *331*, 568.
(37) Matthesis, L. F. *Phys. Rev. Lett.* **1973**, *30*, 784.
(38) Wilcoxon, J.; Thurston, T.; Martin, J. *Nanostruct. Mater.* **1999**, *12*, 993.
(39) Mahan, G.; Sales, B.; Sharp, J. *Phys. Today* **1997**, *50*, 42.